

Electronic supplementary information

Polymer-derived Co/Ni-SiOC(N) ceramic electrocatalysts for oxygen reduction reaction in fuel cells

Thamires Canuto de Almeida e Silva^a, Marek Mooste^b, Elo Kibena-Põldsepp^b, Leonard Matisen^c, Maido Merisalu^{b,c}, Mati Kook^c, Väino Sammelselg^{b,c}, Kaido Tammeveski^b, Michaela Wilhelm^a and Kurosch Rezwan^{a,d}

^a University of Bremen, Advanced Ceramics, Am Biologischen Garten 2, IW3, 28359, Bremen, Germany

^b Institute of Chemistry, University of Tartu, Ravila 14a, 50411 Tartu, Estonia

^c Institute of Physics, University of Tartu, W. Ostwald Str. 1, 50411 Tartu, Estonia

^d MAPEX Center for Materials and Processes, University of Bremen, 28359, Bremen, Germany

Table S1 Composition of PDC-based electrocatalysts (wt%).

Catalyst material composition (wt%)	H44	MK	Graphite	MoSi ₂	Azo	Imi	Ni/CoCl ₂
PDC	21	21	31	8	18	1	-
PDC-Ni	20	20	29	8	17	1	5
PDC-Co	20	20	29	8	17	1	5

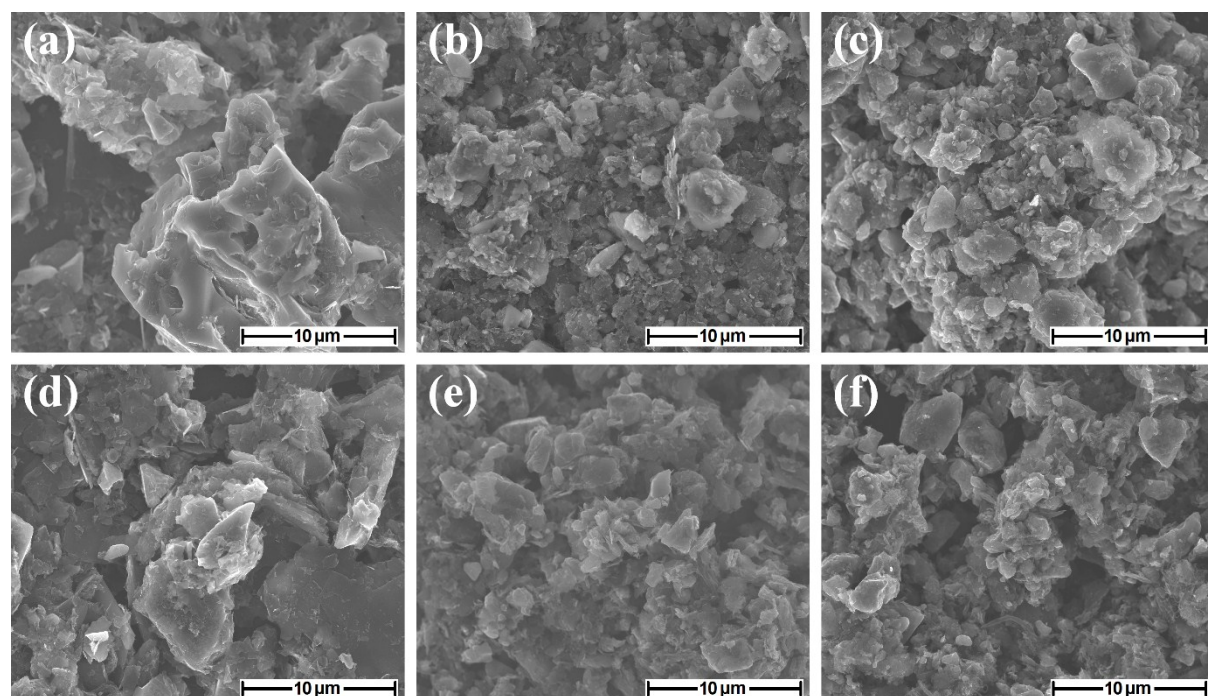


Fig. S1 SEM images (5000 × magnification, scale bar: 10 μm) of (a) PDC, (b) PDC-Ni, (c) PDC-Co, (d) PDC-N, (e) PDC-Ni-N, (f) PDC-Co-N catalyst material on the glassy carbon electrode.

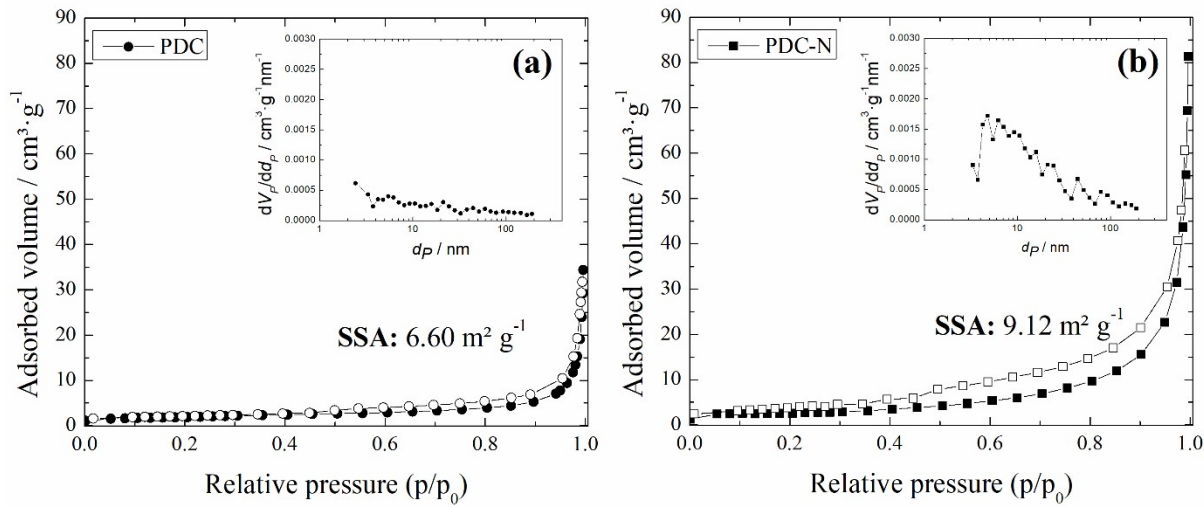


Fig. S2 Nitrogen adsorption-desorption isotherms, respective specific surface areas, and Barrett–Joyner–Halenda (BJH) pore size distribution plot (inset) of the pristine PDC (a) and PDC-N material (b).

Table S2 Pore characteristics and electrical conductivities of the PDC-based electrocatalysts.

Catalyst material	BET SSA (m ² g ⁻¹)	Pore volume (cm ³ g ⁻¹)	Average pore size (nm)	σ (S cm ⁻¹)
PDC	6.6	3.1×10^{-2}	18.8	0.039
PDC-Ni	6.2	1.4×10^{-2}	9.2	0.063
PDC-Co	7.9	2.9×10^{-2}	14.5	0.085
PDC-N	9.1	8.0×10^{-2}	35.2	0.030
PDC-Ni-N	32.3	0.21	25.7	0.030
PDC-Co-N	27.3	0.18	26.2	0.031

Table S3 Elemental composition (at.%) determined from EDX and XPS analysis of the PDC-based electrocatalysts, respectively.

Electrocatalyst	Si	O	C	N	Mo	Ni	Co
EDX results							
PDC	6.4	23.7	67.5	2.3	0.1	-	-
PDC-Ni	5.5	20.3	71.1	2.4	0.3	0.3	-
PDC-Co	6.7	21.0	69.1	2.1	0.4	-	0.4
PDC-N	9.5	22.2	60.9	7.0	0.1	-	-
PDC-Ni-N	5.3	18.1	70.1	5.8	0.3	0.1	-
PDC-Co-N	6.6	15.6	70.7	6.0	0.3	-	0.3
XPS results							
PDC	3.3	8.1	88.6	-	-	-	-
PDC-Ni	9.3	11.2	79.3	-	-	0.2	-
PDC-Co	7.2	13.7	78.9	-	-	-	0.2
PDC-N	2.8	7.3	87.1	2.8	-	-	-
PDC-Ni-N	5.7	8.4	80.6	5.1	-	0.2	-
PDC-Co-N	6.9	10.2	75.7	7.0	-	-	0.2

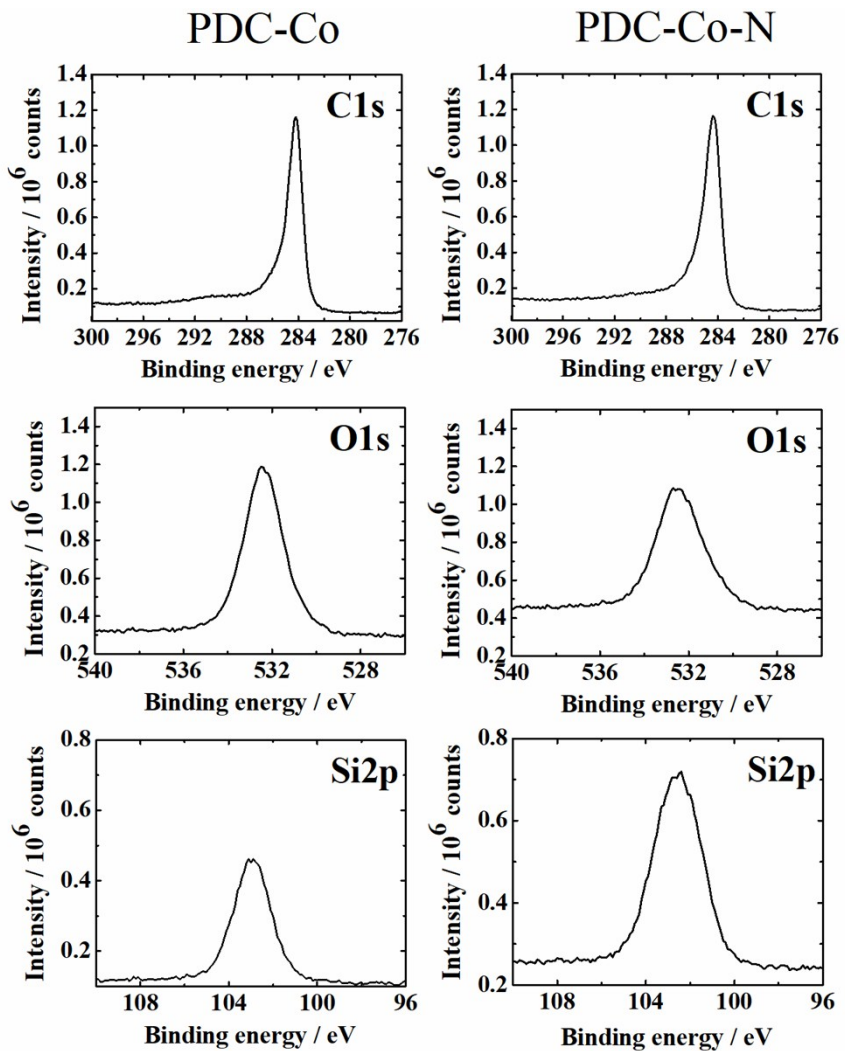


Fig. S3 XPS high resolution spectra in the C1s, O1s and Si2p regions for PDC-Co and PDC-Co-N catalyst materials.

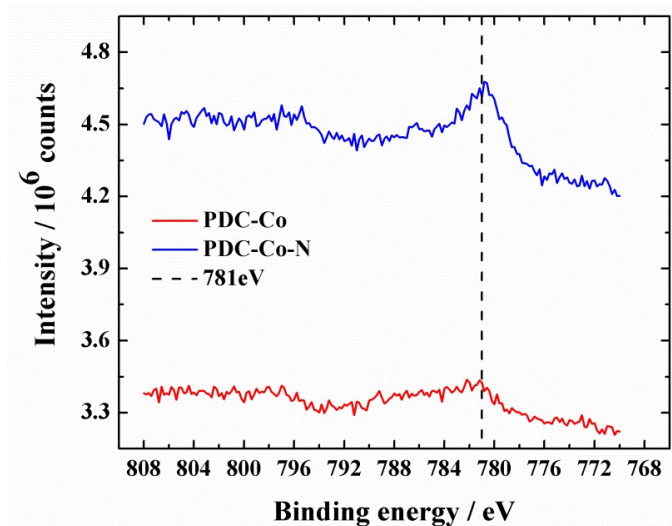


Fig. S4 XPS high resolution spectra in the Co2p region for PDC-Co and PDC-Co-N catalyst materials.

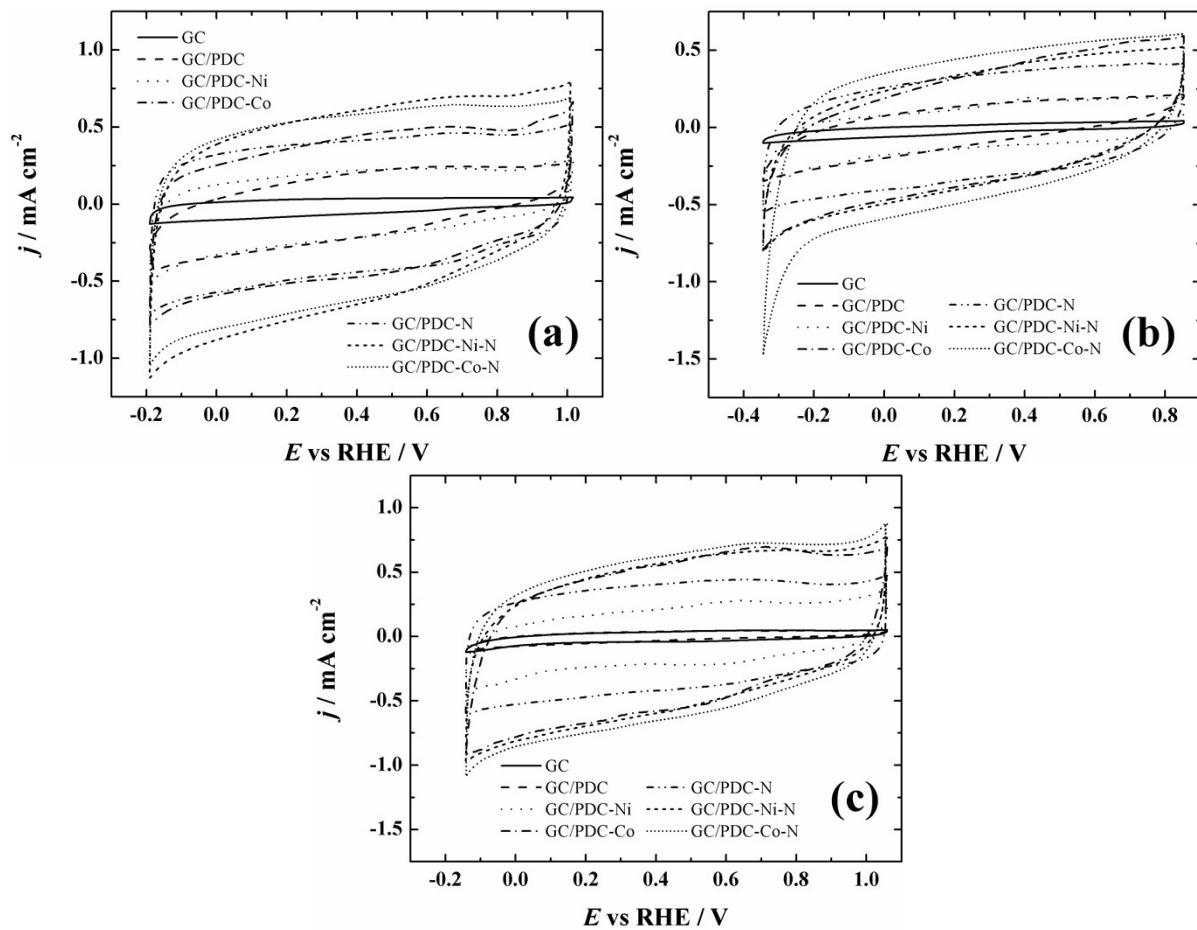


Fig. S5 Cyclic voltammograms of bare glassy carbon and GC electrodes coated with different PDC-based catalyst materials recorded in Ar-saturated 0.1 M KOH (pH = 13) (a), 0.1 M PBS containing 0.1 M NaClO₄ (pH = 7) (b) and 0.5 M H₂SO₄ (pH = 0.3) (c) at $v = 100 \text{ mV s}^{-1}$.

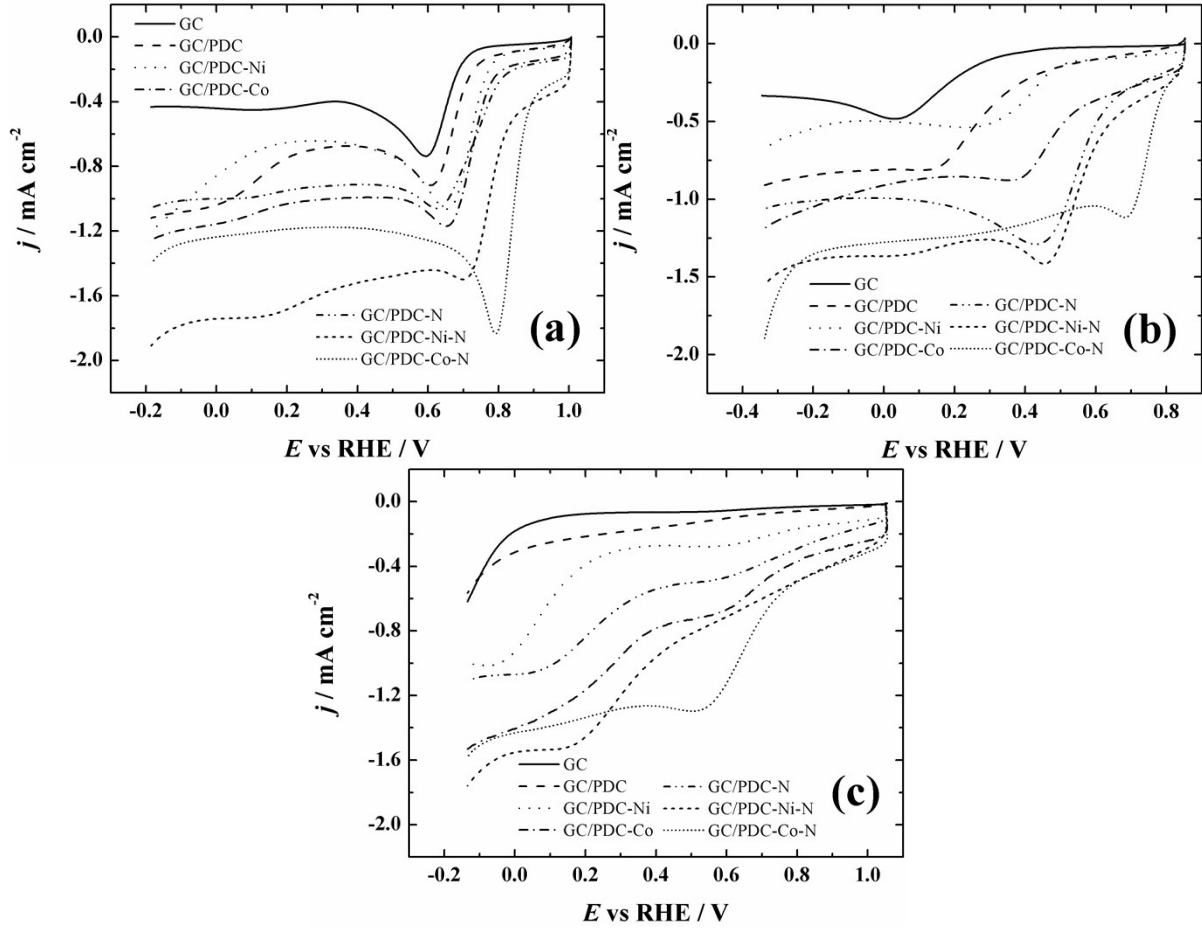


Fig. S6 Linear sweep voltammograms for oxygen reduction on bare glassy carbon and GC electrodes coated with different PDC-based catalyst materials recorded in O_2 -saturated 0.1 M KOH ($pH = 13$) (a), 0.1 M PBS containing 0.1 M $NaClO_4$ ($pH = 7$) (b) and 0.5 M H_2SO_4 ($pH = 0.3$) (c) at $v = 100 \text{ mV s}^{-1}$.

Table S4 The ORR onset potential (E_{onset}), half-wave potential ($E_{1/2}$) and O_2 reduction current density at -0.2 V (j) for different electrodes in O_2 -saturated aqueous solutions. The data is derived from the RDE polarisation curves presented in Figs. 5a, c, e. Experiments were carried out using $\omega = 1900 \text{ rpm}$ and $v = 10 \text{ mV s}^{-1}$. All the potentials are given with respect to the RHE.

Catalyst	$E_{\text{onset}}^{\text{a}}$ (V)	$E_{1/2}^{\text{a}}$ (V)	j^{a} (mA cm $^{-2}$)	$E_{\text{onset}}^{\text{b}}$ (V)	$E_{\text{onset}}^{\text{c}}$ (V)
GC	0.70	0.58	-3.1	0.22	-0.03
GC/PDC	0.73	0.56	-4.0	0.34	-0.05
GC/PDC-Ni	0.78	0.63	-4.7	0.48	0.20
GC/PDC-Co	0.80	0.64	-5.1	0.55	0.38
GC/PDC-N	0.83	0.61	-5.7	0.62	0.38
GC/PDC-Ni-N	0.85	0.62	-6.3	0.63	0.43
GC/PDC-Co-N	0.90	0.80	-6.0	0.79	0.71
Pt/C	0.99	0.86	-	0.97	0.93

^aData obtained in 0.1 M KOH ($pH = 13$) (see Fig. 5a)

^bData obtained in 0.1 M PBS containing 0.1 M $NaClO_4$ ($pH = 7$) (see Fig. 5c)

^cData obtained in 0.5 M H_2SO_4 ($pH = 0.3$) (see Fig. 5e)

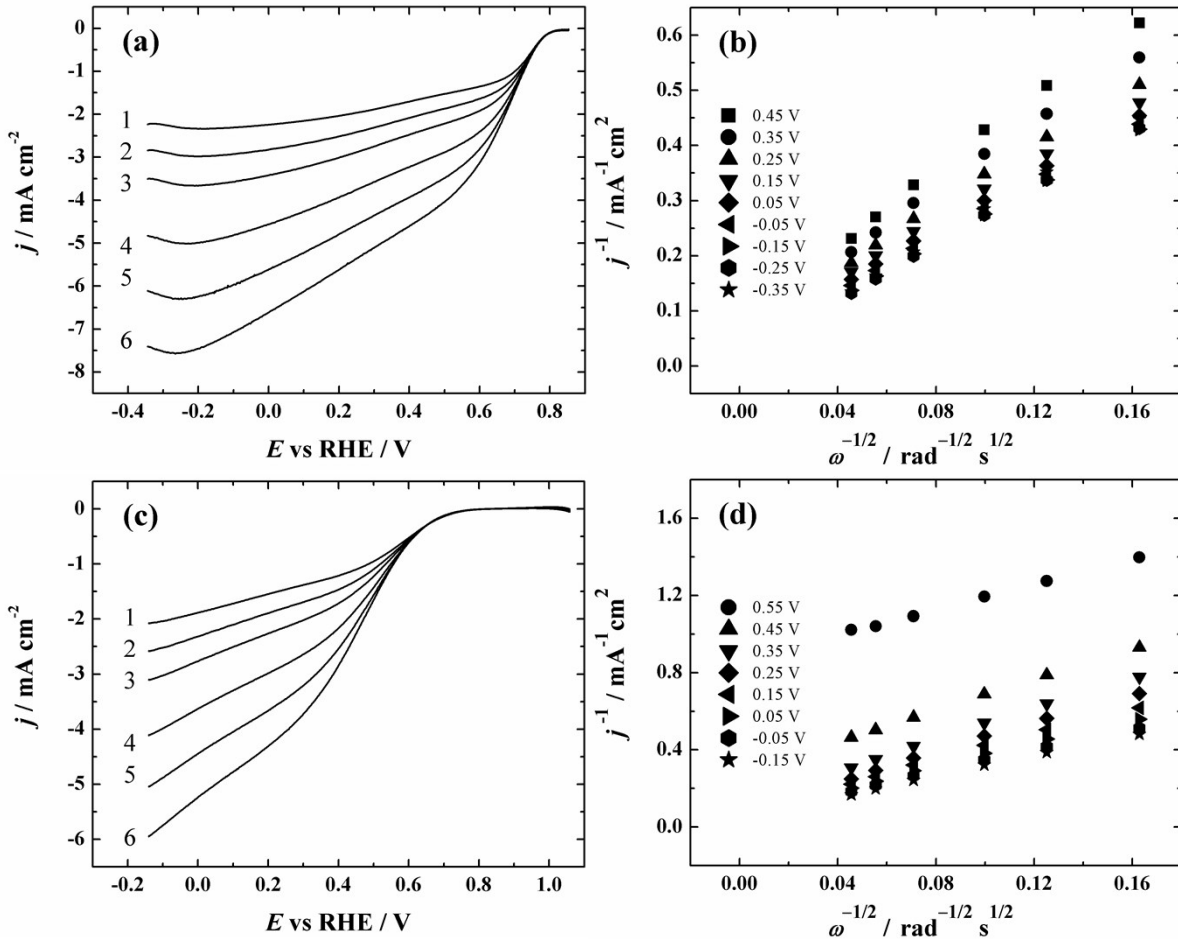


Fig. S7 RDE voltammetry curves for oxygen reduction on GC/PDC-Co-N electrode in O_2 -saturated 0.1 M PBS containing 0.1 M NaClO_4 (pH = 7) (a) and $0.5\text{ M H}_2\text{SO}_4$ (pH = 0.3) (c) (ω : 1-360; 2-610; 3-960; 4-1900; 5-3100; 6-4600 rpm, $v = 10\text{ mV s}^{-1}$). Koutecky-Levich plots for O_2 reduction in 0.1 M PBS containing 0.1 M NaClO_4 (pH = 7) (b) and $0.5\text{ M H}_2\text{SO}_4$ (d) derived from the RDE data shown in Fig. S7a and S7c, respectively.

Table S5 Comparison of the ORR onset potential (E_{onset}), half-wave potential ($E_{1/2}$) and electron transfer number (n) in O₂-saturated 0.1 M KOH for different Co- and N-codoped catalyst materials prepared by pyrolysis. All the potentials are given with respect to the RHE.

Catalyst material (and preparation procedure)	Catalyst loading (mg cm ⁻²)	E_{onset} (V)	$E_{1/2}$ (V)	n	Ref
GC/PDC-Co-N (Polymer-derived Co-SiOC ceramic nanomaterial sonicated along with DCDA and further pyrolysed at 800 °C in N ₂ flow.)	0.2	0.90	0.80	4	This work
Co@NCNT-700 (Synthesized via one-step pyrolysis of CoCl ₂ ×6H ₂ O and DCDA.)	0.2	0.89	-	3.9	1
Co₁₅-N-C800 (Pyrolysis of 1-ethyl-3-methyl-imidazolium dicyanamide and Co(NO ₃) ₂ , later purification by refluxing in 2M H ₂ SO ₄ solution.)	0.49	0.97	0.82	4	2
Co-NCA (Sol-gel polymerisation of organic precursors, followed by insertion of Co by ion exchange and subsequent carbonisation.)	0.2	0.91	0.80	4	3
Co-N-OMMC-0.6 (Dual-templating synthesis in a one-pot controllable procedure by the use of silica colloidal crystal (opal) as a macroporous mold and copolymer as a mesoporous template.)	0.22	-	0.83	3.9	4
Co/N/CDC (Synthesised via pyrolysis of titanium carbide derived carbon, DCDA and CoCl ₂ .)	0.1	0.96	-	4	5
Co_{0.2}-N_{2.35}/C_{0.25}-800 (DCDA and Co(OAc) ₂ ×4H ₂ O mixed, then C-material (BP2000, Cabot) was added and the mixture pyrolysed for 2 h under N ₂ flow.)	-	0.93	-	4	6
NCN-Co-0.1 (Corn starch, DCDA and Co(OAc) ₂ ×4H ₂ O were dissolved in water and after drying pyrolysed in Ar flow.)	0.28	0.93	0.82	4	7
CoNPs@NG (CoCl ₂ , glucose and DCDA heated to 1000° C and held at that temperature for 1 h under N ₂ flow.)	0.25	1.06	1.01	4	8
Co/N/MWCNT-1 (Pyrolysis of CoCl ₂ , DCDA and MWCNTs at 800°C under inert conditions.)	0.1	0.96	0.84	4	9
Co/N-C-800 (Solution of Co(Ac) ₂ , dopamine hydrochloride and NH ₄ OH was mixed and stirred. Firstly, hydrothermal reaction in autoclave, after that carbonisation at 800°C under Ar flow.)	0.25	0.83	-	4	10
Co-NCNT/NrGO-800 (Graphene oxide (GO), CoCl ₂ ×6 H ₂ O and melamine were mixed, stirred and dried. The resulting solid was ground and calcined in two steps (550 and 800 °C) in N ₂ flow.)	0.14	0.91	0.82	3.9	11
NiCo₂O₄-rGO (NiCo ₂ O ₄ nanocrystals grown on reduced GO sheets through polyol process together	0.4	0.88	-	3.8	12

with a thermal annealing at 300 °C in air.)					
Co/N-HCOs ($\text{Co}(\text{CH}_3\text{COO})_2 \times 4\text{H}_2\text{O}$ was added to 2,6-bis(benzimidazol-2-yl)pyridine solution in ethanol. Formed yellow precipitate was washed, dried and heat-treated at 800 °C in N_2 atmosphere.)	0.27	0.92	0.81	4	13
Co@C-NCNTs (N-doped carbon nanotubes decorated with carbon-coated Co nanoparticles prepared by carbonisation at 800 °C and subsequent leaching in HF solution for 12 h.)	0.2	0.86	0.80	4	14
Co-N/Co-O@N-C (N-C prepared by pyrolysis at 900 °C in N_2 flow from copolymers. N-doped hollow carbon microspheres with cobalt nitrate and N-C heated at 300 °C for 1 h in air.)	0.2	0.93	-	4	15
Co-N/G 600 (Hydrothermal process using 2,4,6-triaminopyrimidine, GO and cobalt (II) acetate at 180 °C. Subsequent carbonisation in N_2 atmosphere at 600 °C.)	0.24	0.85	0.76	4	16
Co@C-N-120-900 (D-glucose and cobalt acetate tetrahydrate were added into the g- C_3N_4 (prepared from urea) solution, further hydrothermal treatment 120 °C, final calcination at 900 °C in Ar flow.)	0.2	0.96	0.85	4	17
Co-N/CNFs (Electrospun material from polyacrylonitrile, 4-dimethylaminopyridine and cobalt acetate solution in dimethylformamide. Material stabilised at 250 °C in air, after that pyrolysed in N_2 atmosphere at 950 °C.)	0.2	0.92	0.82	4	18
Co-N-pCNs (Polymerisable ionic liquid $[\text{HVim}]NO_3$ was mixed with the ethanol solution of $\text{Co}(\text{NO}_3)_2$, then dried and pyrolysed at 600 °C in N_2 flow, later treated in 0.5 M HNO_3 .)	0.26	0.96	0.80	3.9	19
Co-NGX 900 (Cobalt acetate, urea, melamine and formaldehyde were added to aqueous dispersion of GO and stirred. Firstly, hydrothermal treatment in autoclave and subsequent pyrolysis at 900 °C in Ar atmosphere.)	0.28	0.97	0.84	4	20
N/Co/CMK-3 plate (The solution in water of ordered mesoporous carbon (CMK-3) and $\text{Co}(\text{NO}_3)_2$ was ultrasonicated and dried. Further, the material was pyrolysed under NH_3 at 800 °C.)	0.14	0.88	0.77	3.9	21

References

1. Y. C. Hao, Z. Y. Lu, G. X. Zhang, Z. Chang, L. Luo and X. M. Sun, *Energy Technol-GER*, 2017, **5**, 1265-1271.
2. Y. D. Qian, Z. Liu, H. Zhang, P. Wu and C. X. Cai, *ACS Appl. Mater. Interfaces*, 2016, **8**, 32875-32886.
3. A. Sarapuu, L. Samolberg, K. Kreek, M. Koel, L. Matisen and K. Tammeveski, *J. Electroanal. Chem.*, 2015, **746**, 9-17.
1. Y. C. Hao, Z. Y. Lu, G. X. Zhang, Z. Chang, L. Luo and X. M. Sun, *Energy Technol-GER*, 2017, **5**, 1265-1271.
2. Y. D. Qian, Z. Liu, H. Zhang, P. Wu and C. X. Cai, *ACS Appl. Mater. Interfaces*, 2016, **8**, 32875-32886.
3. A. Sarapuu, K. Kreek, K. Kisand, M. Kook, M. Uibu, M. Koel and K. Tammeveski, *Electrochim. Acta*, 2017, **230**, 81-88.
4. T. T. Sun, L. B. Xu, S. Y. Li, W. X. Chai, Y. Huang, Y. S. Yan and J. F. Chen, *Appl. Catal., B*, 2016, **193**, 1-8.
5. S. Ratso, I. Kruusenberg, M. Käärik, M. Kook, L. Puust, R. Saar, J. Leis and K. Tammeveski, *J. Power Sources*, 2018, **375**, 233-243.
6. R. Zhang, L. Liu, J. Zhang, W. Y. Wang, F. Ma, R. F. Li and L. Z. Gao, *J. Solid State Electrochem.*, 2015, **19**, 1695-1707.
7. Q. P. Zhao, Q. Ma, F. P. Pan, J. H. Guo and J. Y. Zhang, *Ionics*, 2016, **22**, 2203-2212.
8. L. B. Lv, T. N. Ye, L. H. Gong, K. X. Wang, J. Su, X. H. Li and J. S. Chen, *Chem. Mater.*, 2015, **27**, 544-549.
9. I. Kruusenberg, D. Ramani, S. Ratso, U. Joost, R. Saar, P. Rauwel, A. Kannan and K. Tammeveski, *ChemElectroChem*, 2016, **3**, 1455-1465.
10. Y. H. Su, Y. H. Zhu, H. L. Jiang, J. H. Shen, X. L. Yang, W. J. Zou, J. D. Chen and C. Z. Li, *Nanoscale*, 2014, **6**, 15080-15089.
11. C. T. Wei, H. J. Wang, K. Eid, J. Kim, J. H. Kim, Z. A. Alothman, Y. Yamauchi and L. Wang, *Chem. Eur. J.*, 2017, **23**, 637-643.
12. G. Q. Zhang, B. Y. Xia, X. Wang and X. W. Lou, *Adv. Mater.*, 2014, **26**, 2408-2412.
13. S. J. Chao, Z. Y. Bai, Q. Cui, H. Y. Yan, K. Wang and L. Yang, *Carbon*, 2015, **82**, 77-86.
14. R. Li, X. Z. Wang, Y. F. Dong, X. Pan, X. G. Liu, Z. B. Zhao and J. S. Qiu, *Carbon*, 2018, **132**, 580-588.
15. K. J. Lee, D. Y. Shin, A. Byeon, A. Lim, Y. S. Jo, A. Begley, D. H. Lim, Y. E. Sung, H. S. Park, K. H. Chae, S. W. Nam, K. Y. Lee and J. Y. Kim, *Nanoscale*, 2017, **9**, 15846-15855.
16. Q. Wang, W. H. Hu and Y. M. Huang, *Int. J. Hydrog. Energy*, 2017, **42**, 5899-5907.
17. A. Q. Zhu, P. F. Tan, L. Qiao, Y. J. Liu, Y. Ma, X. Xiong and J. Pan, *Inorg. Chem. Front.*, 2017, **4**, 1748-1756.
18. Q. Q. Cheng, L. J. Yang, L. L. Zou, Z. Q. Zou, C. Chen, Z. Hu and H. Yang, *ACS Catal.*, 2017, **7**, 6864-6871.
19. J. Gao, N. Ma, Y. M. Zheng, J. F. Zhang, J. Z. Gui, C. K. Guo, H. Q. An, X. Y. Tan, Z. Yin and D. Ma, *ChemCatChem*, 2017, **9**, 1601-1609.
20. D. L. Yu and X. Q. He, *J. Appl. Electrochem.*, 2017, **47**, 13-23.
21. V. M. Bau, X. J. Bo and L. P. Guo, *J. Energy Chem.*, 2017, **26**, 63-71.